

# INTERACTION BETWEEN CREEP AND THERMO-MECHANICAL FATIGUE OF CM247LC-DS

C. C. ENGLER-PINTO Jr. <sup>1</sup>, C. NOSEDA <sup>2</sup>, M. Y. NAZMY <sup>2</sup> and F. RÉZAI-ARIA <sup>1</sup>

1) Swiss Federal Institute of Technology, MX-D Ecublens, CH-1015 Lausanne, Switzerland

2) ABB Power Generation Ltd., Materials Technology, CH-5401 Baden, Switzerland

## Abstract

The interaction between creep and thermo-mechanical fatigue (TMF) is investigated on the CM247LC-DS alloy. Out-of-phase TMF tests are performed between 600°C and 900°C on tubular specimens (1 mm wall). Creep rupture experiments are conducted at 900°C on the *virgin* (as received) alloy under 280 MPa on both solid and tubular specimens. Sequential creep-TMF and TMF-creep experiments are performed. Creep cavities and internal cracks are initiated on carbides or residual eutectics. In addition, oxidation assisted crack initiation is observed at the surface of the specimens during creep. No noticeable change on the  $\gamma$ - $\gamma'$  structure is observed during TMF cycling. Under creep, however, a  $\gamma'$ -raft structure develops perpendicularly to the stress axis. This  $\gamma'$ -rafting softens the pre-crept alloy and influences its non-isothermal cyclic stress-strain by increasing the inelastic strain. Short cracks initiated during pre-creeping drastically reduce the TMF crack initiation period. On the other hand, short cracks (100 to 300  $\mu\text{m}$  surface crack length) initiated during pre-TMF cycling do not affect the creep lifetime. A linear creep-fatigue damage cumulative law can predict the residual life of TMF specimens which have been pre-crept.

## Introduction

Directionally solidified (DS) nickel-based superalloys are candidate materials for blading of land based gas turbines. The introduction of DS and single-crystal (SC) superalloys has enhanced creep strength, oxidation resistance, temperature capability and turbine blade durability relative to the earlier conventionally cast equiaxed alloys (1, 2). In both SC and DS blades the [001] crystallographic orientation is set parallel to the blade principal axis. As this direction presents the lowest modulus of elasticity, lower thermal stresses are generated during operation.

The life-limiting factors for turbine blades are thermo-mechanical fatigue, creep and oxidation in the airfoil and high temperature low-cycle fatigue in the root section (3). During the transient regimes of start-up and shut-down operations the blades are submitted to low cycle thermo-mechanical fatigue due to the temperature gradients generated by temperature variations or internal air cooling. Rotor blades are also submitted to creep due to centrifugal forces during the stationary regime of operation. Creep damage accumulation at the maximum operation temperatures can alter the TMF resistance, the damage mechanisms and the mechanical behaviour of the alloy. Consequently, the interaction between creep and thermo-mechanical fatigue is of primary importance for the design of advanced DS blades. This paper aims to assess the interaction between thermo-mechanical fatigue and creep on the CM247LC-DS superalloy.

In general, the effect of creep is studied by adding a dwell period to the isothermal (4-6) or non-isothermal fatigue cycle (7, 8). In this investigation a sequential approach consisting of TMF tests on pre-crept specimens and vice-versa is adopted.

## Alloy and experimental procedures

### Alloy

The specimens are taken from CM247LC-DS cast slabs purchased from AETC (UK). The nominal chemical composition of the alloy is given in Table I. The alloy is multi-step heat treated: solutioning (1260°C, 2h) and ageing (1080°C/4h + 870°C/20h). Full solutioning increases the volume fraction of the fine  $\gamma$  precipitates which enhance positively the mechanical properties of the alloy at high temperatures.

Table I Chemical composition of CM247LC-DS (weight percent).

C	Al	Co	Cr	Fe	Ta	Ti	W	Hf
0.073	5.63	9.3	8.1	0.022	3.19	0.7	9.5	1.4

### TMF experiments

TMF tests are performed in air on hollow specimens (7, 9). The dimensions of the specimens are given in Figure 1. The specimens were machined from the DS slabs by electro-erosion with the elongated grains aligned with the specimen's axis. The internal surface of the specimen is honed and the external surface is mechanically polished with different diamond pastes (down to 1  $\mu\text{m}$ ) in the longitudinal direction. The tests are performed in a conventional closed-loop servo-hydraulic testing machine adapted for non-isothermal fatigue experiments. The specimen is heated by a high frequency generator (6 kW, 200 kHz). A bi-color infra-red pyrometer directed to the gauge length of the specimen is used to monitor the temperature.

The TMF test is conducted under total strain control. The minimum ( $T_{\text{min}}$ ) and maximum ( $T_{\text{max}}$ ) temperatures of the out-of-phase cycle are respectively 600°C and 900°C. Linear heating and cooling (10°C/s) cycles are used. Tests start at the mean temperature (750°C) with nil mechanical strain. Some tests were regularly interrupted in order to take replicas of the specimen surface. Details of the testing procedures are given elsewhere (7).

### Creep experiments

In order to determine the creep rupture time at 900°C and 280 MPa, three solid cylindrical specimens (5 mm diameter and 70 mm length) were machined from the DS slabs by electro-erosion along the longitudinal grains. One creep test was also performed on a TMF specimen. A reference creep rupture time ( $t_r$ ) for the virgin alloy is defined as the average of the lifetimes of all tests.

Superalloys 1996

Edited by R. D. Kissinger, D. J. Deye, D. L. Anton, A. D. Cetel, M. V. Nathal, T. M. Pollock, and D. A. Woodford  
The Minerals, Metals & Materials Society, 1996

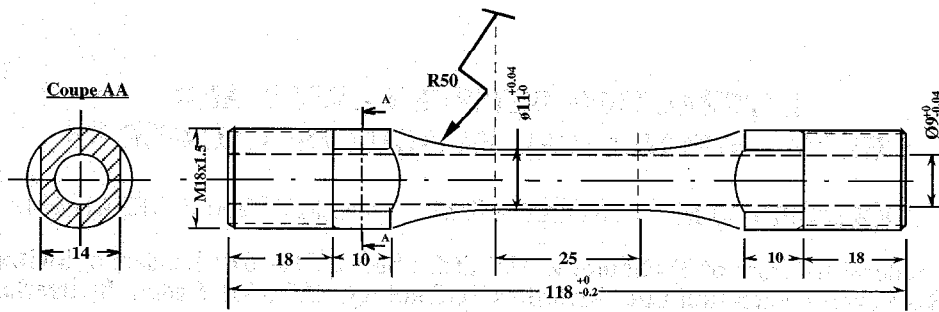


Figure 1: TMF specimen (all dimension in mm).

### Sequential creep and TMF experiments

Tubular specimens are TMF cycled to a certain fraction of life at different mechanical strain ranges and are then crept to total fracture at 900°C and 280 MPa, Table II. The surface of the specimens is not re-polished before final creeping.

Some TMF specimens were pre-crept in tension for 241 h at 900°C and 280 MPa, introducing an inelastic strain of about 1 % to 1.4 %, Table II. After pre-creeping and prior to TMF testing, the internal and external surfaces of the specimens are re-polished in order to suppress the oxide-scale. One pre-crept specimen is used for the determination of the non-isothermal cyclic stress-strain behaviour. Replicas of the external surface were taken after pre-creeping and after pre-TMF cycling.

### Results

#### TMF stress-strain curves

Non-isothermal cyclic stress-strain curves are performed on one virgin and one pre-crept specimen by step increasing of the mechanical strain range. The mechanical strain is increased each time a stabilised hysteresis loop is achieved. The non isothermal stress-strain cyclic curves are reported in Figure 2. The stress and strain ranges measured during the TMF tests at half life are plotted on this graph.

Table II Creep and pre-creeping test results (longitudinal grain).

Temperature, °C	Stress, MPa	Time to rupture, h	Pre-creep time, h	Elongation, %	Specimen
900	280	456	—	26.59	Solid
		472	—	23.10	
		519	—	24.44	
		561	—	21.99	Tubular
		—	241	1.37	Tubular
		—	241	1.40	
—	241	0.92			

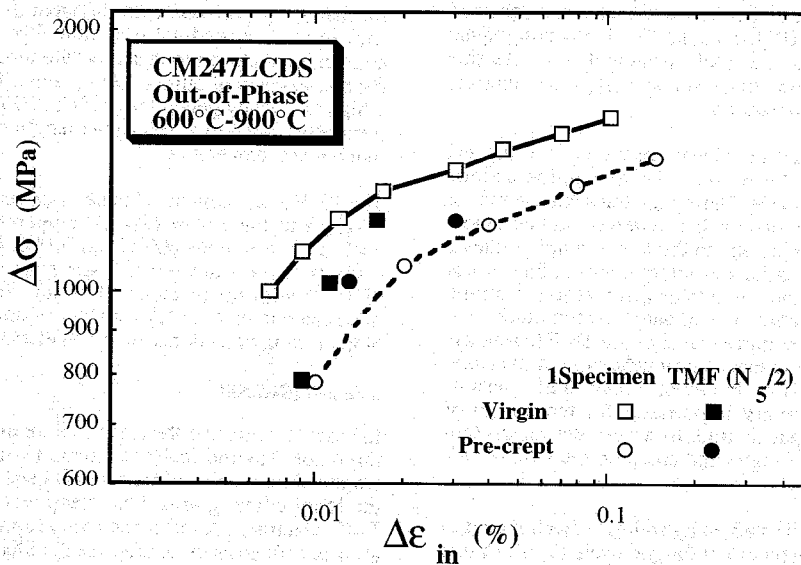


Figure 2: Non-isothermal stress-strain cyclic curves.

TMF-life curves for the virgin and pre-crept conditions

Table III summarises the TMF results obtained for the virgin and pre-crept specimens. The dissipated energy is calculated by numerical integration of the stress-inelastic strain loop at the half life. The TMF life,  $N_5$ , is defined as the number of cycles when a decrease of  $0.05\sigma_{max}$  is observed in the stress range ( $\Delta\sigma$ ). The

crack initiation life  $N_i$  is defined as the number of cycles to form a crack of 0.3 mm at the surface (about 0.1 mm depth).  $N_i$  is obtained by crack measurements on the surface replicas under scanning electron microscopy (SEM).

The TMF life  $N_5$  is plotted as a function of  $\Delta\epsilon_m$ ,  $\Delta\sigma$ ,  $\Delta\epsilon_{in}$  and the dissipated energy respectively in Figures 3 to 8.

Table III Results of the TMF out-of-phase tests on CM247LC-DS.

$T_{max}, ^\circ C$	Alloy	$\Delta\sigma, MPa$	$\sigma_{max}, MPa$	$\Delta\epsilon_m, \%$	$\Delta\epsilon_{in}, \%$	Energy, MJ/m <sup>3</sup>	$N_i$	$N_5$	$N/N_5$ (of virgin)
900	Virgin	794	527	0.8	0.009	0.045	—	12382	1
		1024	838	1.0	0.011	0.061	923	2590	1
		1215	759	1.2	0.016	0.130	510	1125	1
	Pre-crept	1025	711	1.0	0.013	0.088	295	974	0.38
		1208	728	1.2	0.030	0.265	97	631	0.56
	Pre-TMF	1030	664	1.0	0.008	0.076	—	—	0.30
		1025	769	1.0	0.009	0.058	—	—	0.49
		1224	900	1.2	0.010	0.088	—	—	0.51

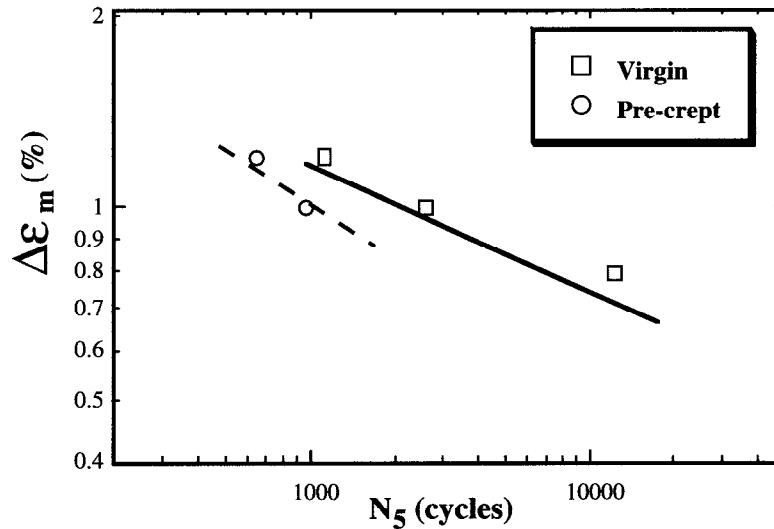


Figure 3: TMF life,  $N_5$ , as a function of mechanical strain range.

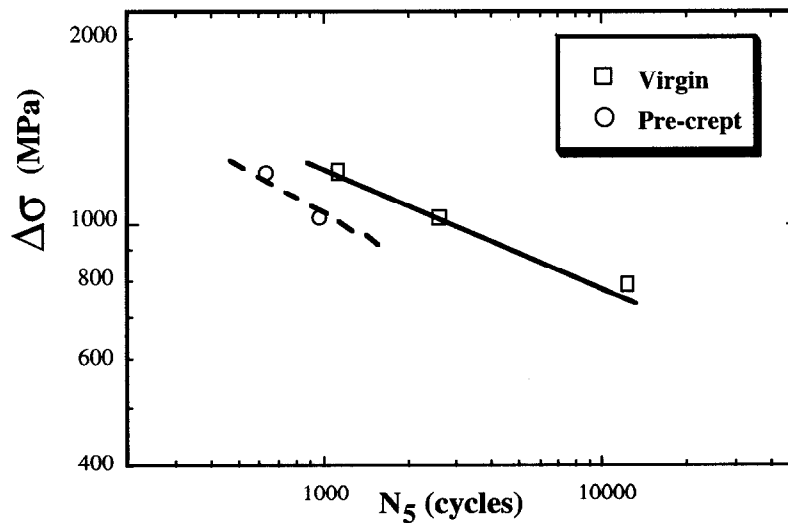


Figure 4: TMF life,  $N_5$ , as a function of stress-range.

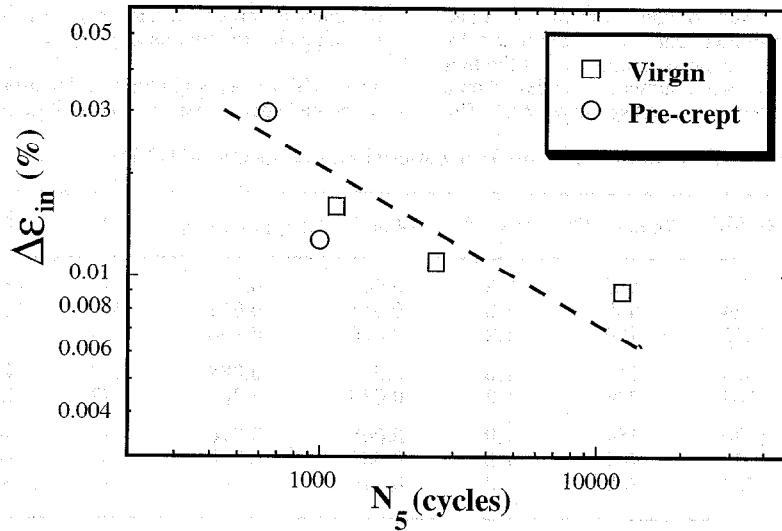


Figure 5: TMF life,  $N_5$ , as a function of inelastic strain range.

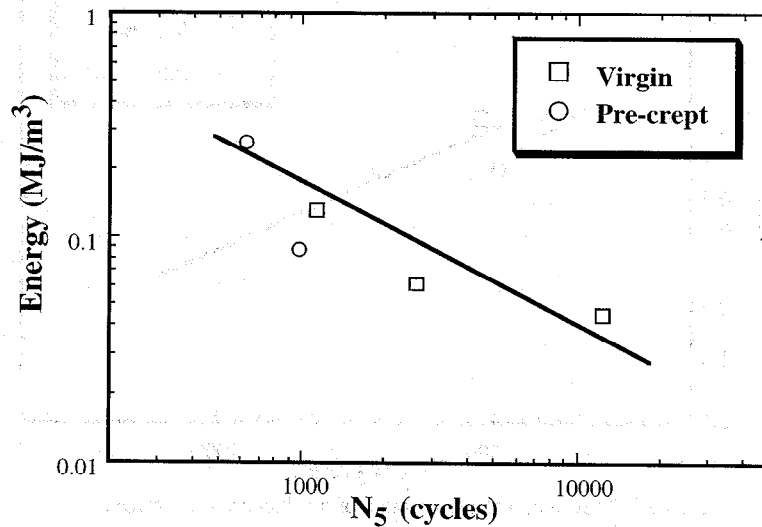


Figure 6: TMF life,  $N_5$ , as a function of dissipated energy.

### Creep

The creep curve of one of the virgin solid specimens is shown in Figure 7. The results of all creep rupture tests are given in Table II. The tubular specimen presents a longer lifetime in comparison to the solid specimens. The mean rupture lifetime ( $t_r$ ) is 502 h.

### Damage mechanisms

SEM observations on the longitudinal sections of solid and tubular specimens after creep reveal that both the bulk and the surface are damaged. In the bulk, cavities nucleate at the interface of carbides or residual eutectics and on fractured carbides. Internal cracks initiate from these cavities. Surface cracks initiate by creep-oxidation interaction process at the grain boundaries. In addition, the  $\gamma'$ -precipitates in virgin alloy (Figure 8a) are rafted perpendicularly to the stress axis (Figure 8b).

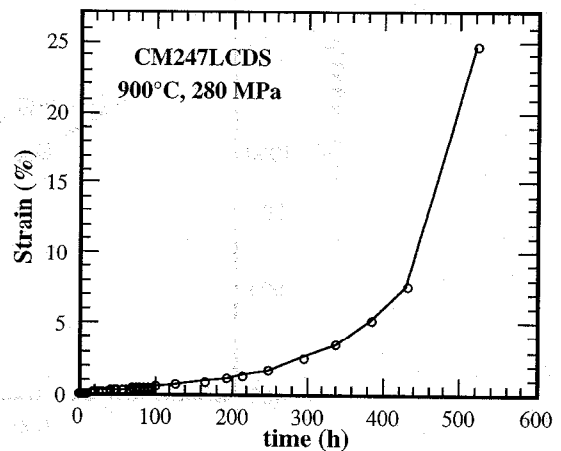


Figure 7: Creep curve of CM247LC-DS at 900°C.

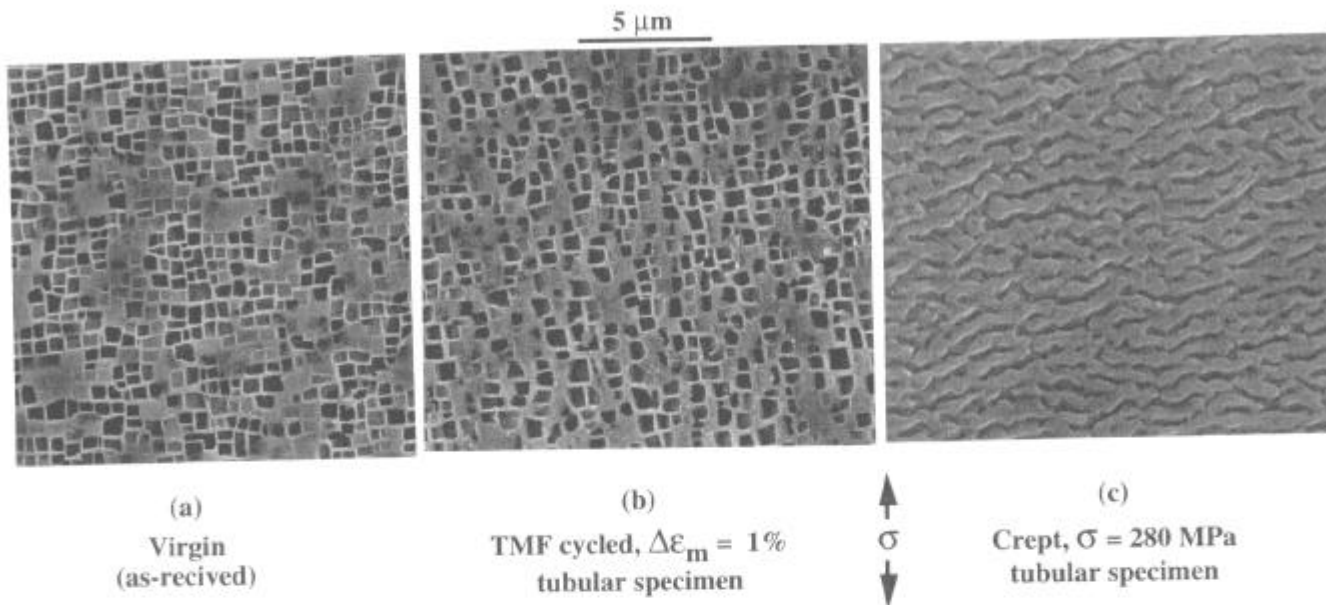


Figure 8: Microstructure of: (a) virgin alloy, (b) after TMF cycling and (c)  $\gamma$ -rafting in crept alloy at  $900^\circ\text{C}$ .

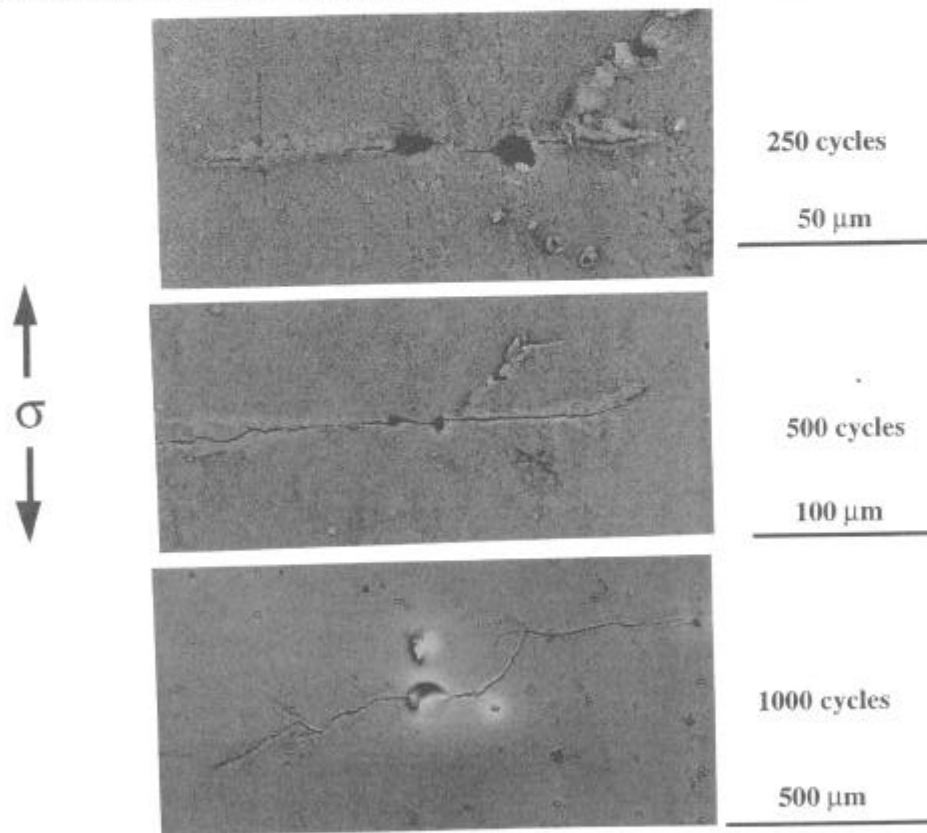


Figure 9: Main crack evolution observed on replicas for the test performed under  $\Delta\epsilon_m = 1.2\%$ .

Observations of the replicas taken from the virgin TMF cycled specimens show that cracks initiate on interdendritic cast porosities. The cracks then propagate in a transgranular manner. Figure 9 shows the evolution of the main crack for the test performed at  $\Delta\epsilon_m = 1.2\%$ . No change is observed on the  $\gamma$ - $\gamma$  structure after TMF cycling (Figure 8c).

#### Discussion

As stated before, a turbine blade is submitted to creep and thermo-mechanical fatigue during each operation cycle. The sequential creep-TMF and TMF-creep procedure adopted in the present investigation is very useful to dissociate the influence of the

damage accumulation introduced in either creep or TMF separately.

Among the various types of damage developed during creep, the surface damage is of primary importance for the residual TMF resistance evaluation. The surface re-polishing has suppressed the oxide scale but has not eliminated the overall damage introduced at the surface during creep (oxide penetration, surface cracks and  $\gamma$  depleted zone). The surface cracks initiated in creep are generally intergranular. These cracks reduce significantly the TMF life of the alloy by reducing the crack initiation period.

It is well known that the high resistance of nickel based superalloys at very high temperatures is due to the  $\gamma$ - $\gamma'$  microstructure. During tensile creep the  $\gamma'$  precipitates on the virgin alloy are rafted perpendicularly to the loading axis. Rafting is observed on alloys which have a negative relative lattice mismatch:  $\delta = 2(a_{\gamma'} - a_{\gamma}) / (a_{\gamma'} + a_{\gamma})$ , where  $a_{\gamma'}$  and  $a_{\gamma}$  are the lattice parameters of the  $\gamma'$  and  $\gamma$  phases (10-12). The internal back stresses developed in  $\gamma$  phase while pre-creeping (12) seems to enhance the inelastic strain under out-of-phase TMF loading (compressive straining while heating) as showed in Figure 2.

It is generally assumed that the fatigue life under isothermal or non-isothermal cycling is governed by the inelastic strain range, Figure 5. The modification of the  $\gamma$ - $\gamma'$  structure (hence the mechanical properties of the alloy) should be considered as an additional parameter which shortens the TMF life. The crack initiation life,  $N_i$ , plotted as a function of the inelastic strain range on Figure 10 clearly demonstrates the effect of pre-creeping on the reduction of the crack initiation period and on the enhancement of the inelastic strain.

Differently to the previous results, pre-TMF cycling has no effect on the creep rupture lifetime. Post-fracture SEM investigations have shown that the initial  $\gamma$ - $\gamma'$  structure of the virgin alloy is not altered by TMF cycling. There are experimental evidences that rafting decreases the creep lifetime of the single crystal superalloys (12). Therefore, one should expect that the creep rupture lifetime

of the CM247LC-DS is not reduced since its microstructure and hence its mechanical properties are not changed by pre-TMF cycling. It should be emphasised, that the short transgranular cracks which initiate from the surface during pre-TMF cycling reduce the creep load bearing section of the specimens but do not influence the creep damage mechanisms.

Figure 11 shows the variation of the residual TMF life,  $N/N_5$ , as a function of the residual creep rupture lifetime,  $t/t_r$ . This figure shows that creep-TMF interactions can be described by a linear damage summation law only when pre-creeping precedes TMF cycling, and not in the reverse case (creep tests on pre-TMF cycled specimens). Therefore, care should be taken when creep-fatigue cumulative damage models are employed for life prediction. It should be emphasised that the synergistic effects of creep and TMF acting simultaneously have yet to be investigated.

### Conclusions

Creep-TMF interaction in CM247LC-DS is investigated. Sequential pre-creeping/TMF cycling and pre-TMF cycling/creeping tests are conducted. The  $\gamma'$ -raft structure developed during creep softens the alloy and enhances the inelastic strain during subsequent TMF cycling. Pre-creeping decreases drastically the TMF life. The main reason for this reduction in life is the initiation of cracks by creep-oxidation interaction, which decrease the TMF crack initiation period. Pre-TMF cycling has no apparent effect on the creep rupture lifetime.

### Acknowledgements

Authors would like acknowledge the Swiss "Commission Pour l'Encouragement de la Recherche Scientifique" for supporting this investigation (project No. 2681.1). Prof. B. Ilschner, the head of the Mechanical Metallurgy Laboratory is very acknowledged for scientific discussions and support.

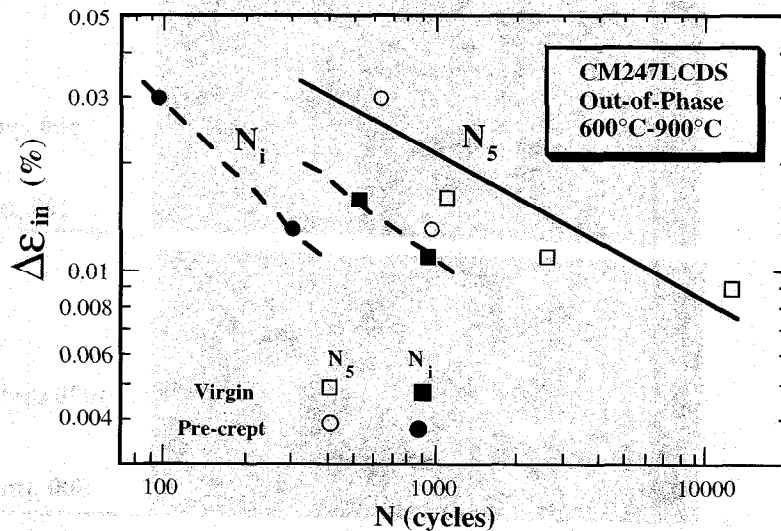


Figure 10: TMF life as a function of the inelastic strain range

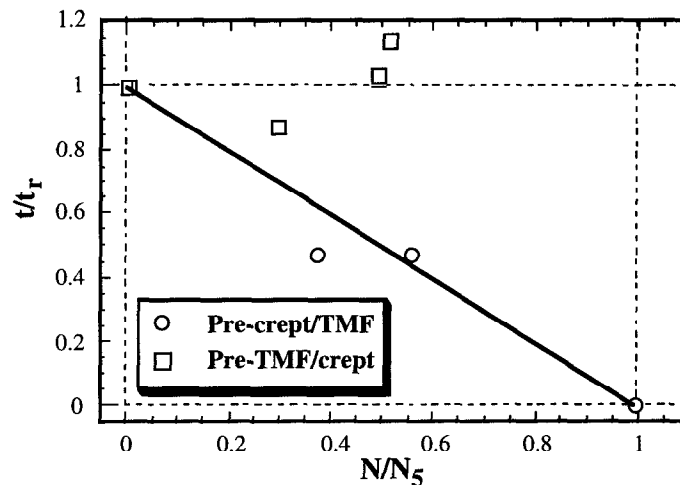


Figure 11: Residual life in creep-TMF interactions.

#### References

1. M. Gell, D. N. Duhl, and A. F. Giamei, "The development of single crystal superalloy turbine blades," (Paper presented at the Fourth International Symposium on Superalloys, Champion, Pennsylvania, USA, 21-25 September 1980), 205-214.
2. K. Harris, G. L. Erickson, and R. E. Schwer, "Development of the CMSX series of single-crystal alloys for advanced technology turbine components," (Paper presented at the TMS-AIME Fall Meeting, St. Louis, Missouri, 1982).
3. C. G. Date et al., "TMF design considerations in turbine airfoils of advanced turbine engines," (Paper presented at the Creep-fatigue interactions at high temperatures, Winter Annual Meeting of the American Society of Mechanical Engineers, ASME, Atlanta, Georgia, 1991), 59-64.
4. C. Levaillant et al., "Creep and creep-fatigue intergranular damage in austenitic stainless steels: discussion of the creep-dominated regime," (Paper presented at the Low Cycle Fatigue, Bolton Landing (on Lake George), New York, 1985), 414-437.
5. L. Rémy et al., "Evaluation of life prediction methods in high temperature fatigue," (Paper presented at the Low Cycle Fatigue, Bolton Landing (on Lake George), New York, 1985), 657-671.
6. P. Rodriguez, K. Bhanu, and R. Sankara, "Nucleation and growth of cracks and cavities under creep-fatigue interaction," *Progress in Materials Science*, Vol. 37 (1993), 403-480.
7. C. C. Engler-Pinto Jr et al., "Thermo-mechanical fatigue behaviour of IN738LC," (Paper presented at the Materials for Advanced Power Engineering 1994, Liège, Belgium, October 3-6 1994), 853-862.
8. G. T. Embley and E. S. Russell, "Thermal mechanical fatigue of gas turbine bucket alloys," (Paper presented at the First Parsons International Turbine Conference, Dublin, Ireland, June 1984), 157-164.
9. J. L. Malpertu and L. Rémy, "Influence of test parameters on the thermal-mechanical fatigue behaviour of a superalloy," *Metallurgical Transactions A*, Vol. 21A (Feb. 1990), 389-399.
10. A. Fredholm and J. L. Strudel, "On the creep resistance of some nickel base single crystals," (Paper presented at the Superalloys 1984, Champion, Pennsylvania, USA, 1994), 211-220.
11. H. Biermann et al., "Internal stresses, coherency strains and local lattice parameter changes in a creep-deformed monocrystalline nickel-base superalloy," *High Temperature Materials and Processes*, Vol. 12 (Nos. 1-2) (1993), 21-29.
12. H. Mughrabi, H. Biermann, and T. Ungar, "Creep-induced local lattice parameter changes in a monocrystalline nickel-base superalloy," *Journal of Materials Engineering and Performance*, 2(4) (August) (1993), 557-564.